

## Quantum critical point in a periodic Anderson model

Peter van Dongen<sup>(1)</sup>, Kengshuk Maimuddar<sup>(2)</sup>, Carey Huscroft<sup>(2)</sup>, and Fu-Chun Zhang<sup>(2)</sup><sup>(1)</sup> Institut für Physik, Johannes Gutenberg-Universität, 55099 Mainz, Germany;<sup>(2)</sup> Department of Physics, University of Cincinnati, OH 45221-0011

(May 20, 2019)

We investigate the symmetric Periodic Anderson Model (PAM) on a three-dimensional cubic lattice with nearest-neighbor hopping and hybridization matrix elements. Using Gutzwiller's variational method and the Hubbard-III approximation (which corresponds to the exact solution of an appropriate Falicov-Kimball model in infinite dimensions) we demonstrate the existence of a quantum critical point at zero temperature. Below a critical value  $V_c$  of the hybridization (or above a critical interaction  $U_c$ ) the system is an insulator in Gutzwiller's and a metal in Hubbard's approach, whereas above  $V_c$  (below  $U_c$ ) it behaves like a metal in both approximations. These predictions are compared with the density of states of the d- and f-bands calculated from Quantum Monte Carlo and NRG calculations. Our conclusion is that the half-filled symmetric PAM contains a metal-semimetal transition, not a metal-insulator transition as has been suggested previously.

PACS numbers: 71.10.Fd, 71.10.Ht, 71.27.+a

## I. INTRODUCTION

Heavy fermion systems, whose properties are determined by nearly localized, strongly correlated f-electrons hybridizing with the d-electrons of the conduction band, have been of considerable interest in recent years.<sup>1</sup> The appropriate theoretical description of heavy fermion systems is believed to be the Periodic Anderson Model (PAM). Among other properties of heavy fermions, this model explains the Kondo effect, i.e., the quenching of the magnetic moments of the correlated electrons by the conduction electrons<sup>2</sup>. Recently, using Quantum Monte Carlo (QMC) techniques, Huscroft et al.<sup>3,4</sup> studied a Periodic Anderson model with the dispersion of the hybridization proportional to that of the conduction electrons. Their study demonstrates that, as the temperature is lowered, the spin singlet correlation function of the conduction electrons develops a sharp structure near a critical value of the hybridization. This indicates a very rapid cross-over between a Kondo regime and a regime where the correlated electrons have unquenched moments. The nature of this crossover was also addressed by Held and Bulla,<sup>5</sup> who showed that the Periodic Anderson model under certain assumptions contains a transition equivalent to the Mott-Hubbard metal-insulator transition in the Hubbard model.<sup>6</sup> Since it is clear already from Ref. 5 that one of the assumptions (the strict separation of high- and low-energy scales) is at best only approximately fulfilled, further analytical and numerical studies of this transition in the PAM are clearly called for.

In this paper we study the nature of this Mott-Hubbard-like transition analytically, using both Gutzwiller's variational method<sup>7,8</sup> and the Hubbard-III approximation<sup>9</sup>. We demonstrate that at half-filling there is a quantum critical point as a function of the hybridization strength which separates a Kondo regime from a phase, in which the d- and f-bands are weakly

coupled (in the Hubbard-III approximation) or even completely decoupled (in Gutzwiller's approach). The disappearance of the Kondo peak beyond the quantum critical point is intimately connected to our choice of the model, with a hybridization strength that vanishes at the Fermi surface of the conduction electrons. We also present new results from 3-dimensional QMC calculations in support of the existence of a quantum critical point.

The grand canonical Hamiltonian describing the two-band periodic Anderson model for hybridized d- and f-electrons is

$$H = \sum_k d_k^y d_k^+ + \sum_k V_k (d_k^y f_k^+ + f_k^y d_k^+) + U \sum_i n_{if}^+ \frac{1}{2} n_{if}^- \frac{1}{2} + \sum_i f_i n_{if}^+ \sum_i (n_{if}^- + n_{id}^-) : \quad (1)$$

Here  $d_k^y$  ( $f_k^y$ ) and  $d_k^+$  ( $f_k^+$ ) are the fermionic operators which create and destroy the d-(f-)band electrons of momentum  $k$  and spin  $\pm$ , and  $n_{if}^- = f_i^+ f_i^-$  is the number operator for the f-electrons of spin  $\pm$  at site  $i$ . Furthermore,  $V_k$  is the momentum dependent hybridization term between f- and d-electrons. Following Refs. 3,4, we consider the dispersion of the d-band and the mixing term  $V_k$  to be that of nearest neighbor hopping on a three-dimensional simple cubic lattice (with unit lattice constant) whereas the f-band is taken to be dispersionless:

$$k = 2t [\cos k_x + \cos k_y + \cos k_z] ; \quad (2)$$

$$V_k = 2V [\cos k_x + \cos k_y + \cos k_z] ; \quad (3)$$

$$f = 0 :$$

Here  $t$  and  $V$  are the hopping matrix elements between the d-d- and f-d-bands respectively. In this paper we study the symmetric PAM in which the chemical potential is  $\mu = 0$  and  $\ln f_i = \ln d_i = 1$ .

As pointed out also in Refs. 3,4, there are good reasons for replacing the usual momentum independent hybridization,  $V_k = V$ , by the momentum dependent hybridization (3). It follows from elementary symmetry arguments that the f- and d-orbitals are essentially orthogonal on the same site. The orthogonality of f- and d-orbitals on the same site implies that the hybridization is predominantly built up from nearest and further neighbor contributions. Our choice (3), which assumes only nearest neighbor contributions to the hybridization, reflects this fact in the simplest possible manner. As shown below, this momentum dependence of the hybridization has important consequences, in particular for physical properties beyond the quantum critical point.

This paper is organized as follows. First, in section II, we introduce our two main methods for investigating the PAM, namely Gutzwiller's variational method and the Hubbard-III approximation. Our variational results for the symmetric PAM are presented in section III; our main finding is that the Gutzwiller approach predicts a Brinkman-Rice type metal-insulator transition. Next, in section IV, we study the PAM in the Hubbard-III approximation, which is equivalent to the exact solution of a Falicov-Kimball model in infinite dimensions. The Hubbard-III solution displays rich behavior as a function of the on-site interaction  $U$ , including a resonance at the Fermi level for weak coupling, a metal-semimetal transition at an intermediate-coupling quantum critical point, and weakly coupled d- and f-bands at strong coupling. We then compare the results from the Gutzwiller and Hubbard-III approaches to QMC simulations of the PAM on a three-dimensional lattice and also to infinite-dimensional QMC results and to calculations based on the Numerical Renormalization Group (NRG, see section V). Finally, in sections V I and V II, respectively, we discuss and summarize our results.

## II. METHODS AND MODELS

Traditionally, in particular in the context of the Hubbard model,<sup>6</sup> there are two famous approaches for investigating metal-insulator transitions, namely the variational approach pioneered by Gutzwiller<sup>7</sup> and Brinkman and Rice,<sup>8</sup> and the Green function decoupling scheme developed by Hubbard.<sup>9</sup> Both of these approaches are clearly approximate in nature. Gutzwiller's method predicts the formation of an ever narrower quasiparticle peak, accompanied by a divergence of the effective mass, as the on-site interaction  $U$  approaches a critical value  $U_c^{\text{Gutz}}$  from below. For  $U > U_c^{\text{Gutz}}$ , the Gutzwiller method leads to unphysical results, such as the suppression of all hopping processes and all double occupancies. This method, therefore, is more realistic at weak than at strong coupling. Hubbard's approximation, on the other hand, is generally considered to be more realistic at strong coupling. At weak coupling it predicts the steady decrease of

the number of charge carriers at the Fermi level; however, this mechanism is implemented in such a way that Fermi liquid properties are violated. At strong coupling Hubbard's method predicts band splitting, i.e., the formation of a lower and an upper Hubbard band. Combination of both methods (the Gutzwiller method at weak and Hubbard's approximation at strong coupling) has yielded valuable information on the metal-insulator transition in the Hubbard model. Here we combine both methods in order to shed light on the nature of the metal-insulator transition in the PAM.

To study the ground state properties of the half-filled PAM, Eq. (1), within the Gutzwiller approach, we follow the variational procedure of Rice and Ueda.<sup>7,10,11</sup> These authors considered the PAM with on-site (rather than nearest-neighbor) hybridization. The central aspect of the Rice-Ueda approach is the suppression of doubly occupied f-states. The Gutzwiller-correlated wave function,  $j_{G,i}$ , is for the case of the PAM defined as

$$j_{G,i} = P j_{0,i}; \quad (4)$$

where  $j_{0,i}$  is the wave function for the uncorrelated ( $U = 0$ ) ground state at half-filling, and  $P$  is the Gutzwiller correlator, defined as

$$P = g^{\hat{D}} = \sum_i \frac{1}{1 - (1 - g)\hat{D}_i} : \quad (5)$$

The operator  $\hat{D} = \sum_i n_{if} n_{if\#}$  in Eq. (5) is the double occupancy operator for the f-electrons and  $g$  is a variational parameter. For  $g = 0$ , the operator  $P$  projects all the states onto the subspace without doubly occupied f-sites, whereas  $g = 1$  corresponds to the uncorrelated state. In general  $g$  has to be determined by minimizing the total energy of the system in the correlated state.

For the symmetric PAM, which is the case of interest in this paper, the Gutzwiller correlator  $P$  is treated by renormalizing all hopping processes by a Gutzwiller factor  $q(d)$ , where  $d = D/N$  is the fraction of doubly occupied f-sites and  $N$  is the total number of lattice sites. This approximation, which is alternatively referred to as the "Gutzwiller approximation" or as "semi-classical counting", becomes exact<sup>12</sup> (at least within the Gutzwiller variational approach, not for the PAM-Hamiltonian itself) in the limit of high spatial dimensions ( $d = 1$ ).

The central element in Hubbard's Green function decoupling scheme is the so-called "alloy analogy", in which it is assumed that the down-spins hop while the up-spins are immobile, and vice versa.<sup>13</sup> The Hubbard-III approximation, like the Gutzwiller approach, can be understood as the exact solution of a simplified problem in high spatial dimensions. In the context of the PAM, the immobile nature of one spin species (say the f<sub>#</sub>-spins), interacting with an "alloy" of immobile electrons of opposite spin (here the f<sub>-</sub>-spins), can be described by the following Hamiltonian:

$$\begin{aligned}
H = & \sum_i^X t d_i^y d_j^y + \sum_{i,j}^X V (d_i^y f_{j\#} + f_{i\#}^y d_j^y) \\
& + U \sum_i^X n_{if}^y \frac{1}{2} n_{if\#}^y \frac{1}{2} \\
& + \sum_i^X f n_{if}^y n_{if\#}^y + n_{id}^y : 
\end{aligned}$$

In this simplified model, the  $f$ -electrons form an alloy of immobile spins, since their hybridization with the  $d$ -band vanishes. As a consequence, the  $d$ -electrons are completely decoupled from the rest of the system and can be integrated out. The creation (annihilation) operators for the remaining  $d$ -electrons will simply be denoted by  $d_i^y$  ( $d_i^y$ ) below. Since we consider the symmetric PAM ( $f = 0$ ) at half-filling ( $\langle \rangle = 0$ ), the last two terms in the Hamiltonian drop out, and we are left with

$$\begin{aligned}
H = & \sum_i^X t d_i^y d_j^y + \sum_{i,j}^X V (d_i^y f_{j\#} + f_{i\#}^y d_j^y) \\
& + U \sum_i^X n_{if}^y \frac{1}{2} n_{if\#}^y \frac{1}{2} : 
\end{aligned} \quad (6)$$

This model is very similar to the spinless two-band Falicov-Kimball model, for which the Hubbard-III approximation (in the framework of the Hubbard model) becomes exact in the limit  $d \rightarrow 1$ . Analogously, the appropriate Green function decoupling ("alloy analogy") for the PAM becomes exact in the simplified model (6) in high dimensions. Below, in section IV, we solve the model (6) exactly in  $d = 1$ . In order to obtain meaningful results in this limit, the hopping and the hybridization have to be scaled as  $t = t = Z$  and  $V = V = Z$ , respectively, where  $Z$  denotes the number of nearest neighbors of each lattice site.

Part of the Hubbard-III approximation is the choice of the lattice. Hubbard<sup>9</sup> started from a semi-elliptical density of states (DOS), which corresponds to the Bethe lattice in high dimensions. Below, we follow Ref. 9 and solve (6) on the Bethe lattice. This choice has several advantages, e.g., that the bandwidth is finite in  $d = 1$ , that the DOS near the band edges resembles the DOS on a simple cubic lattice in  $d = 3$ , and that the properties of the DOS can be studied analytically, since one obtains a relatively simple closed equation for the local Green function.

Essentially the same Hamiltonian (6), but now with on-site hybridization, was considered also by Consiglio and Gusmano.<sup>14</sup> These authors referred to the model as the Simplified Periodic Anderson Model (SPAM), a designation that we extend also to the case of more general (in particular nearest-neighbor) hybridization. The method of solution in Ref. 14 was that of Brandt and Mielisch.<sup>15</sup> Here we use an alternative method<sup>16</sup> that is much better suited for the calculation of the DOS on the Bethe lattice.

### III. GUTZWILLER'S VARIATIONAL APPROACH

In the Gutzwiller approximation, the kinetic energy terms of the PAM are mapped to an effective Hamiltonian with a renormalized hybridization. This result was first obtained with the use of semiclassical counting arguments by Rice and Ueda<sup>10,11</sup> (see also Ref. 17), and then put on a solid footing by Gebhard,<sup>12</sup> who showed that this so-called "Gutzwiller approximation" becomes exact in the limit of infinite spatial dimensionality. We recall that Gutzwiller's variational scheme is equivalent to the slave-boson mean-field theory of Kotliar and Ruckenstein<sup>18</sup> at  $T = 0$ . At half-filling, the effective Hamiltonian in the Gutzwiller approach becomes<sup>10,11</sup>

$$H_e = \sum_k^X k d_k^y d_k^y + \sum_k^X V_k (d_k^y f_k + f_k^y d_k) ; \quad (7)$$

with the renormalized hybridization

$$V_k = \frac{q}{q(d) V_k} :$$

Here the renormalization factor  $q(d)$  takes the form<sup>10,11</sup>

$$q = 8d(1 - 2d)$$

and  $d = D/N$  is the fraction of doubly occupied  $f$ -sites. The ground state energy  $E_g$  is now obtained from the expectation value of  $H_e$ ,

$$E_g = \langle H_e \rangle_{d=N} + U d - U = 4 :$$

The effective Hamiltonian is easily diagonalized. For convenience, we set  $t = 1$ , to establish a unit of energy. One then finds two bands, with eigenenergies  $\#_k$ , where  $\#_k = \frac{1}{2}(1 - 1 + 4qV^2)$ . Note that there is no gap between the two bands, and that both bands contribute to the ground state energy. This is in marked contrast to the results for on-site hybridization.<sup>10,11</sup> The result for the ground state energy is:

$$E_g = j_0 j_1 + 32d(1 - 2d)V^2 + U d - U = 4 ; \quad (8)$$

where  $j_0 = \sum_{f_k < 0} f_k = N$  is the ground state energy per lattice site of a completely decoupled  $d$ -band ( $U = V = 0$ ). Minimizing the ground state energy with respect to  $d$  yields

$$d = \frac{1}{4} \left( 1 - \frac{U}{U_c} \frac{1 + (2V)^2}{1 + (2UV = U_c)^2} \right) : \quad (9)$$

Here we introduced the critical value  $U_c$  of the interaction or, equivalently, a critical value  $V_c$  of the hybridization, for which the expectation value (9) of the double occupancy vanishes:

$$U_c = 16V^2 j_0 j_1 ; \quad V_c = \frac{U}{16j_0 j_1} : \quad (10)$$

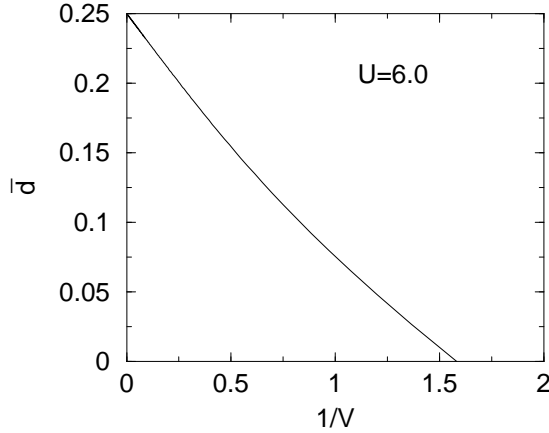


FIG. 1. The fraction of doubly occupied sites is plotted as a function of  $1/V$ , where  $V$  is the hopping between the f- and the d-bands. For the critical  $V_c$ , given in Eq. (10), the number of doubly occupied sites vanishes and all the sites become localized. The parameters are chosen to be  $t = 1$  and  $U = 6$ , and the average energy of the system is calculated by summing over all the filled bands:  $j_0 j = 60 = 4^3$ , where the lattice size is taken to be  $4 \times 4 \times 4$ . With the above values of the parameters the critical value of  $V$  is approximately 0.63.

Since  $d = 0$ , Eq. (9) only applies for  $U = U_c$  (or  $V = V_c$ ). For  $U = U_c$ ,  $d = 0$ . Substituting Eq. (9) into Eq. (8) gives the ground-state energy of the system:

$$E_g = \frac{p}{j_0 j} \frac{1}{[1 + (2V)^2][1 + (2UV = U_c)^2]} : \quad (11)$$

We note that the variational ground-state energy is independent of the hybridization,  $E_g = \frac{U}{4} j_0 j$  for  $U > U_c$ .

In Fig. 1 we plot the fraction of doubly occupied f-sites as a function of the inverse d-f-band hopping parameter  $V$ . The fraction  $d$  decreases monotonically with  $V$  and finally vanishes at a critical value  $V_c$ . This implies that, at this critical value of  $V$ , every f-site is singly occupied, i.e., that the f-electrons are localized.

The critical hybridization strength  $V_c$  (or, equivalently, the critical interaction  $U_c$ ) defines a quantum critical point which separates two distinct regimes in the model. For  $V > V_c$  (or  $U < U_c$ ), the f-electrons hybridize with the d-electrons and their moments are screened. This is the Kondo regime. On the other hand, for  $V < V_c$  (or  $U > U_c$ ), the two bands are decoupled at the Fermi surface, and the f-electron moments are unquenched. Thus the f-electrons show a "metal-insulator transition" from extended ( $U < U_c$ ) to localized ( $U > U_c$ ). In contrast, the d-electrons at the Fermi level are always extended in both regimes.

Following Rice and Ueda,<sup>11</sup> we introduce the binding energy in the Kondo regime as the singular part of the variational ground state energy,

$$E_b(U) = U = 4 j_0 j E_g(U) ;$$

so that  $E_b(U) = 0$  for all  $U > U_c$ . With this definition of the binding energy, it is easy to show that  $E_b$  is positive for all  $U < U_c$ , and that for  $U = U_c$ ,

$$E_b = \frac{2V^2 j_0 j}{1 + 4V^2} \left( 1 - \frac{U}{U_c} \right)^2 \quad (U = U_c) :$$

Near the transition, where the two energy scales  $E_b$  and  $j_0 j$  are well-separated, it seems plausible that  $E_b$  can be identified with the Kondo temperature,  $E_b = k_B T_K$ . It is of interest to compare our result for  $T_K$  to that of Rice and Ueda,<sup>11</sup> who found  $T_K = 2j_0 j e^{U=8V^2}$ . While these results cannot be compared in detail (since Ref. 11 assumes a one-dimensional, linear dispersion for the d-electrons), it is nevertheless clear that the Kondo temperature in our model is strongly suppressed relative to that of Ref. 11 for  $U < U_c$ .

The density of states of the PAM in the Gutzwiler approach is of interest, too. If we denote the DOS of a decoupled d-band ( $U = V = 0$ ) by  $\langle E \rangle$ , then the DOS for the interacting d-electrons in the Gutzwiler approximation is simply given by

$$d(E) = \frac{\langle E = \#_+ \rangle + \langle E = \#_j \rangle}{\#_+ + \#_j} :$$

Thus one finds that the DOS of the d-electrons near the transition ( $U < U_c$ ) is strongly enhanced at the Fermi level compared to the situation for  $U > U_c$ , where  $d(E) = \langle E \rangle$ . This result represents an interesting counter-example to the exhaustion scenario of Nozieres.<sup>19</sup> At low temperatures ( $T < T_K$ ) only the electrons within  $T_K$  of the Fermi surface can effectively participate in screening the local moments. In a concentrated system such as ours, there are more moments to screen than conduction-band states available for screening. In the metallic regime of the conventional PAM, this should lead to a depletion of the density of screening states at the Fermi surface.<sup>20,21</sup> However, within the Gutzwiler approximation this "exhaustion physics" is clearly absent, as we see an enhancement of the d-band DOS near the Fermi surface.

Similarly the f-band DOS takes the form

$$f(E) = \frac{\langle \#_+ = \#_j \rangle \langle E = \#_j \rangle + \langle \#_j = \#_+ \rangle \langle E = \#_+ \rangle}{\#_+ + \#_j} :$$

Thus, in the Gutzwiler approximation, the quasiparticle peak has width  $\#_j / q / d / (1 - U = U_c) / (j_0 j T_K)^{1/2}$ , which is much larger than the Kondo scale  $T_K$ . Hence, interestingly, the Kondo temperature  $T_K$  near the transition is not determined by the width of the peak in the f-DOS, but rather by the (much smaller) binding energy  $E_b$ . The physical explanation for this is that screening becomes increasingly less efficient as one approaches the transition, due to the renormalization of the hybridization rates,  $V_k = \frac{p}{q} \bar{V}_k \neq 0$  for  $U = U_c$ .

#### IV . T H E H U B B A R D - I I I A P P R O A C H

The Hubbard-III approach (alloy analogy) is equivalent to the exact solution in  $d = 1$  of the Simplified Periodic Anderson Model (SPAM), Eq. (6) with  $t = t = \frac{1}{2}$  and  $V = V = \frac{1}{2}$ . For the calculation of the DOS on the Bethe lattice, it is most convenient to map the SPAM to an effective non-interacting Hamiltonian, following the lines of Ref. 16, and then use the renormalized perturbation expansion<sup>22</sup> to calculate the DOS. This method also allows one to conclude immediately that the DOS at half-filling is temperature independent, as a consequence of the non-interacting nature of the effective Hamiltonian. Along the lines of Ref. 16 we find that the Fourier transform of the local matrix Green function,

$$G_{ii}(z) = \frac{hT}{2} \frac{d_i^y(0)i}{f_{i\#}(0)i} \frac{hT}{2} \frac{d_i^y(0)i}{f_{i\#}(0)i} ;$$

satisfies a cubic matrix equation,

$$G(z) = \frac{1}{2} \left[ \begin{array}{cc} 1 & G \\ G & 1 \end{array} \right]^{-1} + \left[ \begin{array}{cc} 0 & G \\ G & 0 \end{array} \right]^{-1} ; \quad (12)$$

with

$$I(z) = \begin{vmatrix} z & 0 \\ 0 & z - \frac{1}{2}U \end{vmatrix} ; \quad = \begin{vmatrix} t & V \\ V & 0 \end{vmatrix} ;$$

In spite of the formally simple structure of Eq. 12, the detailed analysis of the DOS of the d- and f-electrons is rather involved and will be published elsewhere.<sup>23</sup> Here we focus on the physical content of the Hubbard-III results and compare them to results from the Gutzwiler approach and various numerical techniques. For convenience we put  $t = 1$  to fix the unit of energy; note that this convention differs from that of the previous section.

#### A . D ensity of states at strong interaction

First we consider the results from the Hubbard-III approximation in the limit of large interaction,  $U \gg 1$ . In this limit almost all the spectral weight of the d-electrons is contained in a semi-elliptic band near  $E = 0$ :

$$d(E) = \frac{1}{2} \frac{p}{4} \frac{1}{E^2} ; \quad (13)$$

Similarly, nearly all spectral weight of the f<sub>#</sub>-electrons is contained in two high and narrow peaks near  $E = \pm \frac{1}{2}U$ , whose width is of order  $V^2 = U$  while their height is proportional to  $U = V^2$ . With a redefinition of the energy variable as  $s = U(E \pm \frac{1}{2}U) = V^2$ , one finds

$$f_{\#}(E) = \frac{U}{4V^2} \frac{p}{6} \frac{1}{1 - s^2} ;$$

provided that the argument of the square root is positive ( $3 - 8 < s < 3 + 8$ ); otherwise  $f_{\#}(E)$  vanishes. The presence of an upper and a lower Hubbard

band in the f<sub>#</sub>-spectrum at first sight suggests the occurrence of a metal-insulator transition at some finite value of  $U$ . However, closer inspection shows that there is some small additional spectral weight for the d-electrons near  $E = \pm \frac{1}{2}U$ ,

$$d(E) = \frac{1}{2U} \frac{p}{6} \frac{1}{1 - s^2} ;$$

and small additional spectral weight for the f<sub>#</sub>-electrons near  $E = 0$ :

$$f_{\#}(E) = \frac{2V^2}{U^2} \frac{p}{4} \frac{1}{E^2} ;$$

This is a first clear indication that the f<sub>#</sub>-electrons in the SPAM do not undergo a metal-insulator transition. Instead one finds a metal-semimetal transition: at arbitrarily large  $U$ , the d- and f<sub>#</sub>-bands remain weakly hybridized.

#### B . D ensity of states at the Fermi level

Exactly at the Fermi level ( $E = 0$ ) an explicit non-perturbative solution can be obtained for all interaction strengths  $U$ . A detailed analysis of the cubic matrix equation (12) shows that there is only one physically acceptable solution,

$$G(0) = \begin{pmatrix} g_1(0) & g_2(0) \\ g_2(0) & g_3(0) \end{pmatrix} ;$$

where the matrix elements of  $G(0)$  are given by

$$\begin{aligned} g_1(0) &= \frac{p}{2iR_+} \\ g_2(0) &= \frac{i}{2V} (R_+ - R_-) \\ g_3(0) &= \frac{i}{2V^2} (R_+ - R_-) ; \end{aligned}$$

and

$$R = \frac{s}{1 - \frac{U^2}{8V^4}} \frac{r}{1 - \frac{U^2}{4V^4}} ;$$

These results hold only for  $U > U_c^{AA} = 2V^2$ , where the superscript "AA" stands for "alloy analogy". For all  $U > U_c^{AA}$  the solution is simply given by  $g_1(0) = i$  and  $g_2(0) = g_3(0) = 0$ . Note that the Hubbard-III and Gutzwiler approaches predict the same dependence of  $U_c$  on the hybridization: both  $U_c^{AA}$  and  $U_c^{Gutz}$  are simply proportional to  $V^2$ .

Physically these results mean, that at weak coupling the DOS at the Fermi level decreases fairly slowly as the interaction  $U$  is switched on, both for the d- and the f<sub>#</sub>-electrons:

$$\begin{aligned} d(0) &= \frac{2}{V^2} \left( 1 - \frac{U^2}{16V^4} \right)^{\frac{9}{2}} & (U \neq 0); \\ f_{\#}(0) &= \frac{1}{V^2} \left( 1 - \frac{U^2}{8V^4} \right)^{\frac{9}{2}}; \end{aligned}$$

while the critical values are approached quite rapidly:

$$\begin{aligned} d(0) &= \frac{1}{V^2} \left( 1 + \frac{p}{U_c^{AA}} \right)^{\frac{9}{2}} & U = V \\ f_{\#}(0) &= \frac{1}{V^2} \left( \frac{p}{U_c^{AA}} - \frac{1}{U} \right)^{\frac{9}{2}} & U = V^3 \end{aligned}$$

For all  $U > U_c^{AA}$  the  $f_{\#}$ -DOS at the Fermi level vanishes exactly, while the d-DOS is pinned at the value  $d(0) = 1$ . This clearly demonstrates that  $U_c^{AA}$  marks a quantum critical point, although the nature of the transition cannot be deduced from an investigation of the DOS only at the Fermi level.

We add that, at weak coupling, the DOS for both the d- and the f-electrons displays an interesting resonance at the Fermi level. This resonance is very narrow, of  $O(U^2)$ , and its height remains of  $O(1)$  for  $U \neq 0$ . The amplitude of the resonance for the d-electrons is positive, so that the d-band DOS at  $U = 0^+$  is larger than for  $U = 0$ . In contrast, the amplitude of the resonance in the f-band is negative, i.e., the f-band DOS at  $U = 0^+$  is smaller than for  $U = 0$ .

### C. Density of states at and beyond the critical point

We now consider the shape of the DOS as a function of energy, first for  $U = U_c^{AA}$  and then for  $U > U_c^{AA}$ . We focus on the energy interval near the Fermi level, since this interval determines the nature of the quantum critical point and virtually all physical properties of interest.

First we present the result for the DOS exactly at the transition, i.e., for  $U = U_c^{AA}$ . In this case one finds that the DOS has a sharp (cubic-root) singularity as a function of energy for  $E \neq 0$ :

$$\begin{aligned} d(E) &= \frac{1}{2} + \frac{p}{2} \left( 1 + \frac{1}{V^2} \right)^{\frac{1}{3}} E^{\frac{1}{3}} & (E \neq 0); \\ f_{\#}(E) &= \frac{p}{2} \left( \frac{1}{V^2} - \frac{1}{E^2} \right)^{\frac{1}{3}} E^{\frac{1}{3}} & (E \neq 0); \end{aligned}$$

Cubic-root critical behavior of the DOS near the Fermi level is well-known from the Hubbard-III solution for the Hubbard model. Here we find that similar critical behavior occurs also for the SPAM with nearest-neighbor hybridization.

For energies near the Fermi level, one generally finds that the d-DOS for  $U > U_c^{AA}$  is metallic while the  $f_{\#}$ -DOS is semimetallic. In particular, one finds that the  $f_{\#}$ -DOS contains spectral weight, arbitrarily close to the Fermi level,

$$f_{\#}(E) = \frac{4V^2}{U^2} E^2 \quad (E \neq 0; U > U_c^{AA});$$

Note that the coefficient in front of the semimetallic  $E^2$ -behavior is valid for all  $U > U_c^{AA}$  and, hence, simply identical to that calculated in section IV A for large  $U$ .

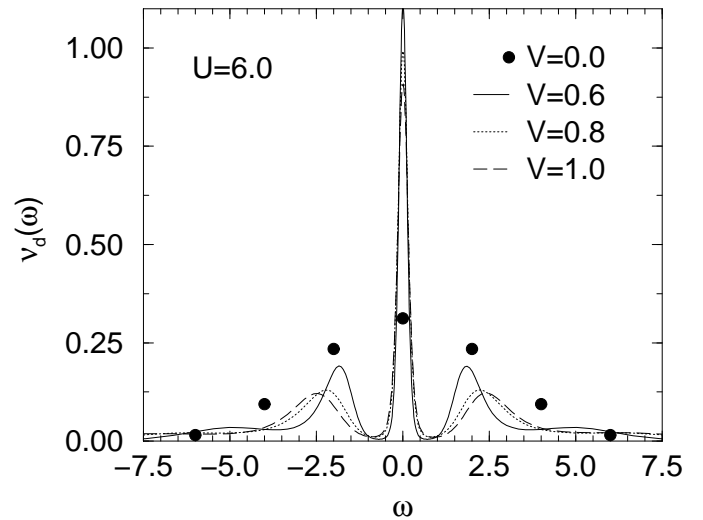


FIG. 2. The d-band density of states,  $v_d(\omega)$ , for the 3d PAM via finite-d QMC for various hybridizations,  $V > V_c$ . The DOS at the Fermi energy is resonantly enhanced over the non-interacting value, shown as dots in the figure. For  $V < V_c$ , the Green function is similar to the non-interacting Green function, which indicates that the d- and the f-bands are approximately decoupled in this regime (not shown).

### V. COMPARISON TO QMC AND NRG RESULTS

To obtain a complete picture of our model, we compare our analytical results to single-particle spectra obtained from three different numerical techniques: (i) QMC simulations of the PAM on a three-dimensional lattice (where we present new results and compare to results from recent<sup>3,4</sup> calculations), (ii) QMC simulations of the PAM on an infinite-dimensional lattice<sup>4</sup>, and (iii) recent results from NRG calculations in infinite dimensions.<sup>5</sup>

We start with the comparison to the three-dimensional QMC results. In Fig. 2 we plot new results for the d-band DOS obtained using the maximum entropy method to analytically continue three-dimensional QMC data calculated at  $T = 0.2$ . For small  $V$  the presence of upper and lower Hubbard bands well separated by a gap  $U$  can be seen in the f-band DOS. With increasing  $V$ , the weight in the central region is enhanced at the expense of the Hubbard side-bands.

For  $V$  larger than the critical hybridization  $V_c$ , the DOS for the d-band is greatly enhanced compared to the non-interacting d-band DOS (shown in dots). This is consistent with the previously mentioned enhancement of the d-band DOS in the Gutzwiller approximation in this regime. On the other hand, in the regime where  $V < V_c$ , the Green function is not significantly different from the non-interacting Green function. This indicates that for  $V < V_c$ , the d-band is weakly coupled to the f-band. This result is compatible with both the Gutzwiller result (that the d-band is strictly  $V$ -independent for  $V < V_c$ , i.e.,  $d(E) = d(0)$ ) and the Hubbard-III result, Eq. 13,

which holds asymptotically both for  $U \gg 1$  and  $V \gg 0$ .

The f-band DOS was studied in Refs. 3,4 with the use of finite- and infinite-dimensional QMC techniques. The infinite-dimensional (DMFT) calculations<sup>4</sup> were also done for a strictly paramagnetic state, without antiferromagnetic fluctuations. For small hybridization,  $V < V_c$ , one finds that the f-band DOS consists primarily of an upper and a lower Hubbard band around  $E = \pm \frac{1}{2}U$ , respectively. Only in the DMFT calculations<sup>4</sup> is there a sign of small spectral weight near the Fermi level. For increasing  $V$ , one finds that the upper and lower Hubbard bands merge. Before the bands merge ( $V < V_c$ ), additional resonant peaks develop, which are characteristic for Kondo singlet formation. After the bands merge ( $V > V_c$ ), the f-band DOS in the infinite-dimensional simulation shows some depletion near the Fermi level. Since this depletion is absent in the DMFT calculations, this feature is most likely due to short-range antiferromagnetic fluctuations. Comparing these numerical results to those from the Hubbard-III and Gutzwiller approaches, we observe that the merging of the two bands is described by the Hubbard-III approach but not by the Gutzwiller approximation. The Hubbard-III approach also explains the small additional spectral weight near the Fermi level in the DMFT calculation. The Gutzwiller approximation cannot explain either the upper and lower Hubbard bands or small spectral weight near the Fermi level. Obviously, neither approach can explain the depletion due to short-range antiferromagnetic fluctuations in the infinite-dimensional calculations.

We add that, very recently, Held and Bulla<sup>5</sup> performed calculations for the paramagnetic ground state of the PAM using the Numerical Renormalization Group (NRG). These calculations clearly reveal significant additional spectral weight near the Fermi level for  $U < U_c$ . The numerical results in Ref. 5 are the clearest evidence to date that the quantum critical point in the PAM corresponds to a metal-semimetal and not to a metal-insulator transition. Interestingly, the authors of Ref. 5 show analytically that the PAM under certain assumptions contains a transition equivalent to the Mott-Hubbard metal-insulator transition in the Hubbard model. However, they also point out that one of these assumptions (the strict separation of high- and low-energy scales) is at best only approximately fulfilled for  $U > U_c$ , especially for larger values of the hybridization rate ( $V > 1$ ). The Hubbard-III results of this paper strongly suggest that the high- and low-energy scales in the PAM are in fact never strictly separated, so that the transition is from a metal to a semimetal, not an insulator. Physically it seems obvious that for large  $U$ , as a result of the finite hybridization rate, the f-band must have some spectral weight near the Fermi level, where the weight of the d-band is concentrated. Similarly, the d-band must have some spectral weight near the upper and lower Hubbard bands of the f-electrons, i.e., near  $E = \pm \frac{1}{2}U$ .

## V I. DISCUSSION

The two main questions to be discussed are: What can be learned from the Gutzwiller and Hubbard-III approximations for the PAM? And what features are missing in these two analytical approximation schemes?

As pointed out before, in section II, one expects Gutzwiller's variational method to be more realistic at weak than at strong coupling. This expectation is based on experience with the Hubbard model and on the fact that the Gutzwiller wave function becomes exact in the weak coupling limit. For similar reasons, Hubbard's approximation is considered to be more realistic at strong coupling. For example, the Hubbard-III approximation violates weak-coupling (Fermi liquid) properties and is, therefore, better suited at strong coupling ( $U > U_c$ ). Combination of these two approaches leads to the following physical picture.

We distinguish high and low spatial dimensions. In high spatial dimensions, short-range antiferromagnetic fluctuations are small, which is a prerequisite for the validity of the Gutzwiller and Hubbard-III approaches. The Gutzwiller approach then shows that the f-band DOS develops a quasiparticle peak near the Fermi level if the interaction  $U$  is turned on. The quasiparticle peak becomes ever narrower, until it vanishes at the critical interaction  $U_c$ , where the metal turns into a semimetal. The Gutzwiller approach is unable to describe the side bands in the DOS that develop for  $U < U_c$ . These high-energy features are better captured by the Hubbard-III approximation which, in turn, is unable to describe the Fermi liquid peak. For  $U > U_c$  one expects the DOS to remain semimetallic, as is seen in the Hubbard-III approach. The Hubbard-III results further suggest that, at some finite interaction  $U > U_c$ , the DOS splits into three parts: a lower Hubbard band near  $E = -\frac{1}{2}U$ , a semimetallic low-energy part of the spectrum, and an upper Hubbard band near  $E = +\frac{1}{2}U$ . This scenario is consistent with the results from the high-dimensional QMC simulations and agrees very well with those of the NRG calculations discussed in section V.

In contrast, there will be significant short-range antiferromagnetic fluctuations in the paramagnetic phase in low spatial dimensions (certainly for  $d = 1, 2$  and to some extent also for  $d = 3$ ). In these dimensions one, therefore, expects depletion of the f-band DOS near the Fermi level. This depletion is explicitly seen in three-dimensional QMC calculations.<sup>3,4</sup> These depletion effects cannot be described in terms of the paramagnetic Gutzwiller wave function for the PAM, since it does not contain the necessary antiferromagnetic fluctuations. The effects of finite-dimensionality on the quality of the Hubbard-III results for  $U > U_c$  is probably not large. One expects the semimetallic part of the DOS to be somewhat depleted in  $d = 3$  as compared to  $d = 1$ . An interesting question that cannot be answered at this stage is, whether the semimetallic pseudogap changes

its functional form due to short-range antiferromagnetic fluctuations and, in particular, whether these fluctuations might turn the pseudogap into a hard gap. Given these uncertainties concerning the influence of antiferromagnetic fluctuations in finite dimensions, it seems fair to say that our results are at least consistent with the three-dimensional QMC data published here and in Refs. 3 and 4. We do not believe that our results can reasonably be applied to one- and two-dimensional systems, since physics in these low dimensions differs too much from that in high dimensions, where our approximations are valid.

In the Gutzwiller and Hubbard-III methods studied in this paper, only states without broken symmetry were considered. The true ground state of the half-filled symmetric PAM, of course, may well be antiferromagnetically ordered.<sup>3,4,24,25</sup> In this sense our results are not so much relevant for the ground state of the PAM, but rather for the paramagnetic phase at slightly elevated temperatures ( $T > T_{\text{Neel}}$ ). With this proviso, we believe that the main result of our paper, the absence of Kondo screening for  $V < V_c$  (or  $U > U_c$ ), is robust. In particular, we expect that metal-semimetal transition, predicted by the Hubbard-III approach, actually occurs in the PAM with nearest-neighbor hybridization.

A comment is in order concerning the critical values of the interaction in the Gutzwiller and Hubbard-III ("alloy analogy") approaches,  $U_c^{\text{Gutz}}$  and  $U_c^{\text{AA}}$ . In sections III and IV we found that  $U_c^{\text{Gutz}} = 16V^2 j_0 \frac{t^2}{1+t^2}$  and  $U_c^{\text{AA}} = 2V^2 = t$ , where we reinstated factors of  $t$  and  $t = t = Z$ . In order to be able to compare these two results, we calculate the critical value  $U_c^{\text{Gutz}}$  for the Bethe lattice with coordination number  $Z = 1$ . One readily finds that in this case  $j_0 j = 8t=3$ , so that  $U_c^{\text{Gutz}} = 128V^2/(3t)$ . Hence there is a significant discrepancy between the two  $U_c$ -values:  $U_c^{\text{Gutz}} = U_c^{\text{AA}} = 64/3 = 6.79$ . Partly this is due to the neglect of "resonance broadening corrections", which are part of the full Hubbard-III approximation but are not taken into account in the alloy-analogy approach.<sup>13</sup> For the Hubbard model, the resonance broadening corrections are known<sup>6</sup> to enhance  $U_c^{\text{AA}}$  by a factor of  $\sqrt{3}$ , so that one then finds a ratio  $U_c^{\text{Gutz}} = (\sqrt{3}U_c^{\text{AA}}) = 32/3 = 1.96$ . Hence the Gutzwiller prediction for  $U_c$  in the Hubbard model is significantly larger than the full Hubbard-III result. In the PAM the discrepancy is even larger. Even if resonance broadening corrections are taken into account through an ad hoc factor of  $\sqrt{3}$ ,  $U_c^{\text{Gutz}}$  is still larger than  $\sqrt{3}U_c^{\text{AA}}$  by a factor of nearly 4. In order to determine which of the three predictions  $U_c^{\text{Gutz}}$ ,  $U_c^{\text{AA}}$  and  $\sqrt{3}U_c^{\text{AA}}$  is best, we compare with results from recent NRG-calculations for the ground state of the PAM in high dimensions.<sup>5</sup> E.g., for  $t = V = 1$  one finds that  $U_c^{\text{PAM}} = 4$ . In conclusion, compared to the NRG-value,  $U_c^{\text{AA}}$  is too small by a factor of 2 due to the neglect of resonance broadening corrections, the "corrected" value  $\sqrt{3}U_c^{\text{AA}}$  is quite close, and the Gutzwiller prediction  $U_c^{\text{Gutz}}$  is too large by a factor

of 3.395. For the PAM, therefore, the full Hubbard-III approximation leads to a much more accurate prediction for the critical interaction than the Gutzwiller approach.

We now comment on the influence of small deviations from the strict nearest-neighbor hybridization,  $V_k^{\text{es}} = 2V \sum_{\sigma=1}^d \cos(k_\sigma)$ , which we considered throughout in this paper. As an example, we consider combinations of this "extended s-wave" form and a local ("s-wave") hybridization,  $V_k^s = V_s$ , or a "p-wave" form,  $V_k^p = 2V_p \sum_{\sigma=1}^d \sin(k_\sigma)$ . In the Gutzwiller approximation, one readily finds that there is now a gap at the Fermi surface and that the renormalization factor  $q$  is now finite for all  $U > 0$ . For instance, one finds for a mixture of an extended s-wave and a s-wave:

$$q / \frac{t^2}{V_s^2} \exp \left( \frac{U - U_c(V)}{16(0)V_s^2} \right) \quad (U > U_c) : \quad (14)$$

For a mixture of an extended s-wave and a p-wave, the factor  $V_s^2$  in the exponent is replaced by the average of  $(V_k^p)^2$  over the non-interacting Fermi surface of the d-electrons. Strictly speaking, Eq. (14) implies that the quantum critical point, which occurs for  $V_s = V_p = 0$ , is unstable with respect to small s- or p-wave perturbations. However, Eq. (14) also shows that the QCP at  $U_c(V) = 16V^2 j_0 \frac{t^2}{1+t^2}$  is replaced by a sharp crossover to a state with very heavy quasiparticles. Experimentally this could hardly be distinguished from the metal-insulator (or metal-semimetal) transition found for  $V_s = V_p = 0$ .

Finally we comment on the difference between the local and nearest-neighbor hybridization rates from a renormalization group point of view. The Kondo effect is due to the antiferromagnetic coupling of d-electrons near the Fermi surface to the f-electron moments. As the system renormalizes, the coupling scales to the strong coupling ( $J = 1$ ) fixed point. Adjacent to this fixed point, only energy scales and moments near the Fermi surface are important. For the standard PAM the hybridization is constant, and one finds the usual Kondo effect. In contrast, the most salient feature of the model we study is that the f-d hybridization vanishes at the Fermi surface of the half-filled non-interacting model, as can be seen from Eqs. (2) and (3). The corresponding exchange coupling also vanishes on the Fermi surface, and therefore cannot be rescaled to the strong coupling limit. Thus the absence of the Kondo effect in our model at small values of  $V=t$  is fully consistent with the usual renormalization group arguments.

## VII. SUMMARY

We have studied the half-filled symmetric Periodic Anderson model with an f-d hybridization proportional to the d-band dispersion, using Gutzwiller's variational wave function and Hubbard's alloy-analogy approach. Both methods demonstrate the occurrence of a quantum phase transition for a critical value  $V_c$  of the f-d

hybridization rate or, equivalently, for a critical interaction strength  $U_c$ . For  $V > V_c$  (or  $U < U_c$ ) the system is a metal. For  $V < V_c$  (or  $U > U_c$ ) the system behaves as an insulator in Gutzwiller's approximation and as a semimetal in the Hubbard-III approach. Based on the results of these two approximation methods, we predict the occurrence of a similar quantum phase transition in the exact solution of the PAM with nearest-neighbor hybridization. A number of the properties of this transition, such as a strong suppression of the Kondo temperature on the metallic side, were also predicted. Most importantly, we conclude from our results that the nature of the transition in the exact solution of the PAM will be that of a metal-semimetal, not a metal-insulator<sup>5</sup> transition. These analytical results are compared with the DOS obtained from QMC simulations and NRG results for the d- and f-bands. We find good agreement between our scenario and QMC- or NRG-results in high spatial dimensions ( $d = 1$ ), while our results are at least consistent with the QMC-calculations published here and in Refs. 3 and 4 for the three-dimensional PAM.

#### ACKNOWLEDGMENTS

We acknowledge important and very helpful discussions with Prof. Mark Jarrell (Univ. of Cincinnati). This work was supported by PRF (KM, FZ) and the NSF grant DMR-9704021 (CH, KM). We thank the U.S. Dept. of Energy ASCI program for supercomputer time for the QMC simulations.

ingredients. Apart from the "alloy analogy", there is also the "resonance broadening" correction, which attempts to restore the mobility of the alloy-spins. Since resonance broadening cannot be understood in terms of a control parameter (like high dimensionality), and since it leaves the qualitative features of the transition unchanged, we focus on the alloy analogy. However, we return to the influence of "resonance broadening" corrections in the Discussion.

- <sup>14</sup> R. Consiglio and M. A. Gusman, Phys. Rev. B 55, 6825 (1997).
- <sup>15</sup> U. Brandt and C. M. Eisenschitz, Z. Phys. B 75, 365 (1989).
- <sup>16</sup> P. G. J. van Dongen, Phys. Rev. B 45, 2267 (1992).
- <sup>17</sup> D. Vollhardt, Rev. Mod. Phys. 56, 99 (1984).
- <sup>18</sup> G. Kotliar and A. Ruckenstein, Phys. Rev. Lett. 57, 1362 (1986).
- <sup>19</sup> P. Nozieres, Eur. Phys. J. B 6, 447 (1998).
- <sup>20</sup> A. N. Tahvildar-Zadeh, M. Jarrell, and J. K. Freericks, Phys. Rev. B 55, R3332 (1997).
- <sup>21</sup> A. N. Tahvildar-Zadeh, M. Jarrell, Th. Pruschke, and J. K. Freericks, to appear in Phys. Rev. B 60.
- <sup>22</sup> E. N. Economou, Green's Functions in Quantum Physics (Springer-Verlag, Berlin, 1979).
- <sup>23</sup> P. G. J. van Dongen, to be published.
- <sup>24</sup> M. Jarrell, Phys. Rev. B 51, 7429 (1995).
- <sup>25</sup> P. Coleman, Physica B 259-261, 353 (1999).

<sup>1</sup> P. A. Lee, T. M. Rice, J. W. Serene, L. J. Sham, and J. W. Wilkins, Comments Cond. Mat. Phys. 12, 99 (1986).

<sup>2</sup> A. C. Hewson, "The Kondo Problem to Heavy Fermions," Cambridge Univ. Press, Cambridge (1993).

<sup>3</sup> C. Huscroft, A. K. M. Mahan, and R. T. Scalettar, Phys. Rev. Lett. 82, 2342 (1999); A. K. M. Mahan, C. Huscroft, R. T. Scalettar, and E. L. Pollock, J. Comput. Aided Mater. Design 5, 131 (1998).

<sup>4</sup> K. Held, C. Huscroft, A. K. M. Mahan, and R. T. Scalettar, preprint (1999).

<sup>5</sup> K. Held and R. Bulla, cond-mat/0006418 preprint.

<sup>6</sup> F. Gebhard, The Metal-Metal-Insulator Transition (Springer, Berlin, 1997).

<sup>7</sup> M. C. Gutzwiller, Phys. Rev. 137, A1726 (1965).

<sup>8</sup> W. F. Brinkman and T. M. Rice, Phys. Rev. B 2, 4302 (1970).

<sup>9</sup> J. Hubbard, Proc. Roy. Soc. London A 281, 401 (1964).

<sup>10</sup> T. M. Rice and K. Ueda, Phys. Rev. Lett. 55, 995 (1985).

<sup>11</sup> T. M. Rice and K. Ueda, Phys. Rev. B 34, 6420 (1986).

<sup>12</sup> F. Gebhard, Phys. Rev. B 44, 992 (1991).

<sup>13</sup> The full Hubbard-III approximation<sup>9</sup> actually contains two